Single-cell transcriptomic analysis of experimental ischemic brain injury in time and space

Abaffy P.[1], Žucha D.[1], Kirdajová D.[2], Benešová Z.[1], Anděrová M.[2], Valihrach L.[1]

1 Laboratory of Gene Expression, Institute of Biotechnology CAS, BIOCEV Vestec, Czech Republic; 2 Department of Cellular Neurophysiology, Institute of Experimental Medicine CAS, Prague, Czech Republic;
e-mail: pavel.abaffy@ibt.cas.cz

Introduction

Nervous tissue reacts to ischemic brain injury with complex machinery of molecular and cellular processes that prevent additional tissue damage. However, these processes also result in forming problematic scar-like tissue, which acts like a barrier for repair of damaged brain environment. A better understanding of mechanisms governing cell response to ischemic brain injury is therefore crucial for effective design of new treatment strategies. In this study, we used several high-throughput methods to study spatiotemporal changes of brain environment after middle cerebral artery occlusion in mouse model. These methods includes single-nucleus RNA sequencing and spatially resolved gene expression analysis (spatial transcriptomics). We compared three time points (1 day, 3 days and 7 days after surgery) with sham control.

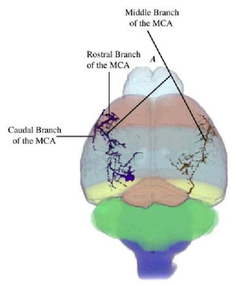

1. Middle cerebral artery of left hemisphere was occluded.

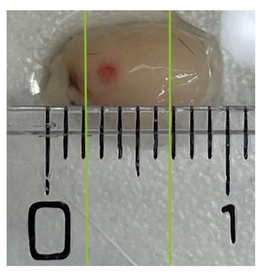

2. Left hemispheres (region separated by green lines) were collected into O.C.T. (spatial transcriptomics) or directly frozen on dry ice (single-nucleus RNA-seq).

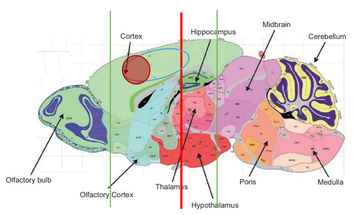

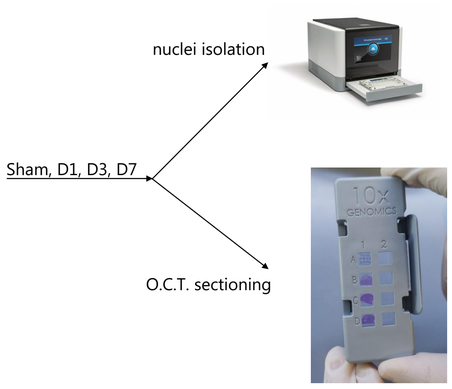

3. Nuclei were isolated from fresh frozen tissue and single-nucleus RNA-Seq libraries were prepared using 10x Chromium Controller. O.C.T. embedded tissues were sliced using cryostat and mounted on 10x Visium Slide. Hematoxylin & Eosin staining was used prior library preparation.

Results

Identification of major cell types in mouse brain

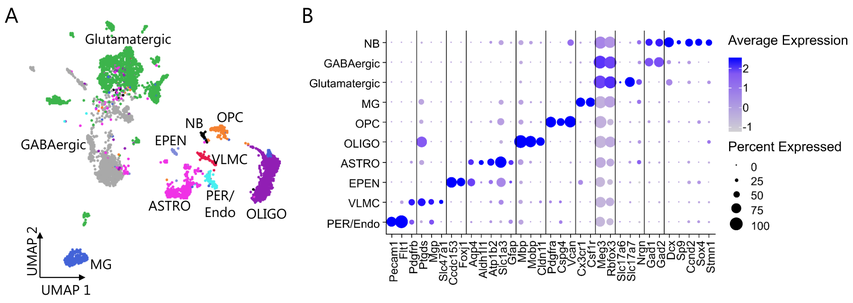

Fig. 1. Annotation of clusters of main cell types. Ten major populations were identified. (**A**) UMAP plot with annotated cell types. (**B**) Dot plot is showing expression level of known markers of main cell types of mouse brain.

PER – pericytes; Endo – endothelial cells; VLMC – vascular leptomeningeal cells; EPEN – ependymal cells; ASTRO – astrocytes; OLIGO – oligodendrocytes; OPC – oligodendrocyte progenitor cells; MG – microglia; NB – neuroblastema cells;

Ischemia-specific subpopulations

Astrocytes

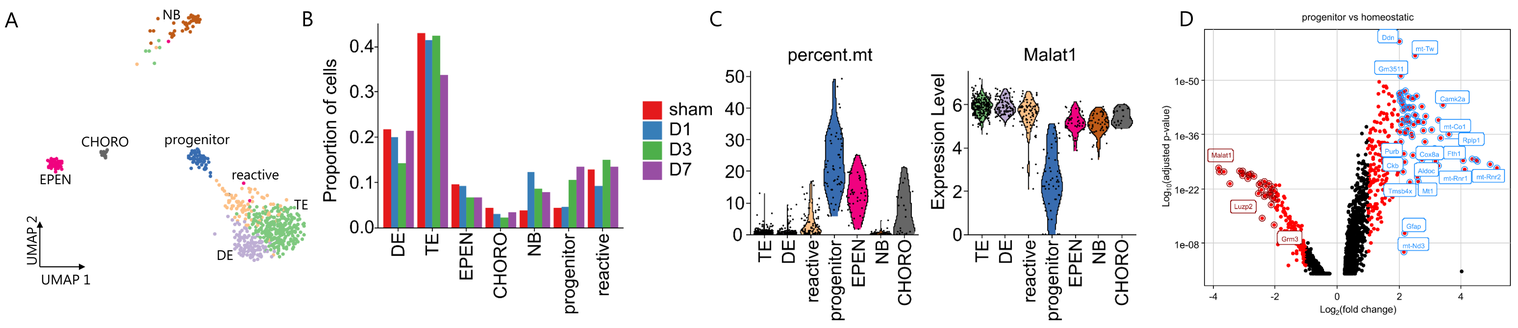

Fig. 2. Subclusters of astro-ependymal cells identified in mouse ischemic brain. Seven different populations were identified, while proportion of two of them increased after ischemia in comparison with sham control. (**A**) UMAP plot with annotated subclusters. (**B**) Proportion of subclusters in each time point. Proportion of neuroblastema and progenitor cells increase over the time. (**C**) Astrocyte progenitor cells have higher content of mitochondrial RNA in nuclei. However, expression level of *Malat1* (specific gene for low quality cells/nuclei) is lower in comparison with other subclusters. (**D**) Top DEGs in progenitors of astrocytes in comparison with homeostatic (diencephalic and telencephalic) are mitochondria specific genes and neuronal specific genes.

DE – diencephalic astrocytes; TE – telencephalic astrocytes; EPEN – ependymal cells; CHORO – choroid plexus specific cells; NB – neuroblastema cells;

Oligodendrocytes

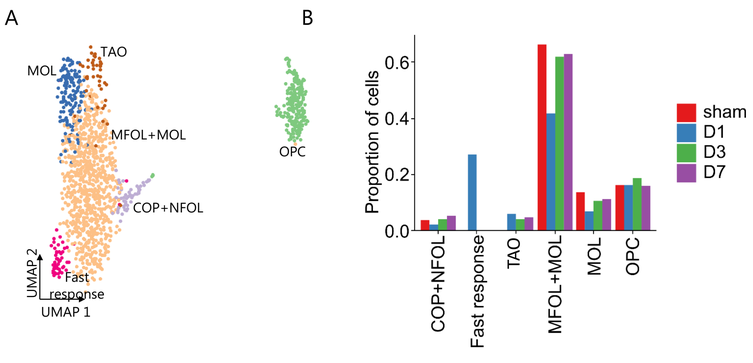

Microglia

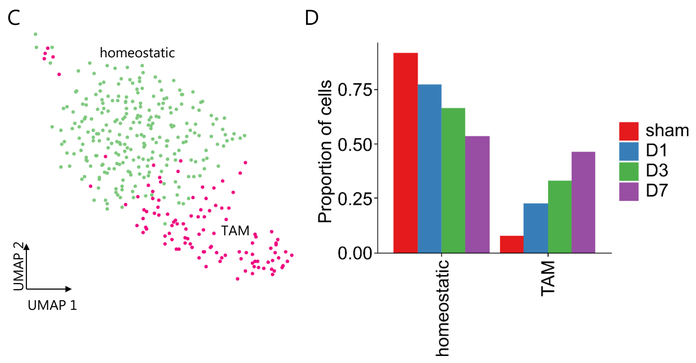

Fig. 3. Subclusters of oligodendrocytes and microglia identified in mouse ischemic brain. Six different populations of oligodendrocytes and two different populations of microglia were identified. Two populations of oligodendrocytes were observed only in murine ischemic brain and proportion of one population of microglia increased after ischemia. (**A**, **C**) UMAP plot with annotated subclusters of (**A**) oligodendrocytes and (**C**) microglia. (**B**, **D**) Proportion of subclusters in each time point. (**B**) Fast response oligodendrocyte were observed only in day 1 and trauma associated oligodendrocytes (TAO) were observed only after ischemia. (**D**) Proportion of trauma associated microglia (TAM) increases over the time.

OPC – oligodendrocyte precursor cells; COP – committed oligodendrocyte progenitors; NFOL – newly formed oligodendrocytes; MFOL – myelin forming oligodendrocytes; MOL – mature oligodendrocytes; TAO – trauma associated oligodendrocytes; TAM – trauma associated microglia

Annotation of main brain regions

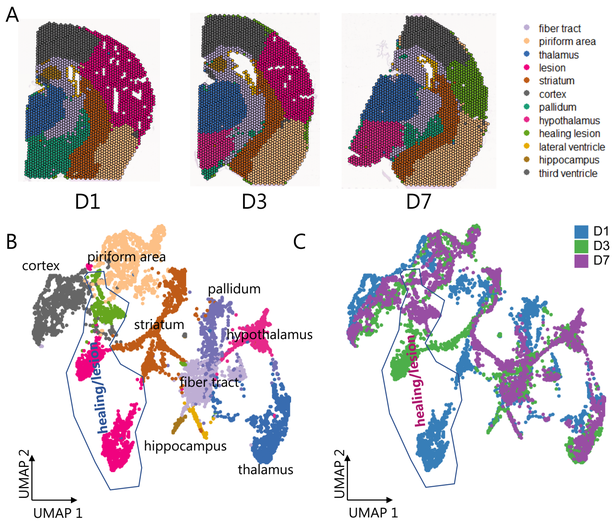

Fig. 4. Identification of main mouse brain regions. Regions were clustered based on the gene expression profiles and named based on their localization. Lesion is observed only in cortex and piriform area and does not include area of striatum. (**A**) Spatial plot of clustered spots. (**B**, **C**) UMAP plot of spots coloured based on the (**B**) region specific annotation or (**C**) condition. Spots from lesion/healing parts cluster separately from the regions of origin (Day 1), while they are getting closer to them in later time points (Day 3 and Day 7).

Identification "healthy" populations which are accumulated in the damaged brain region

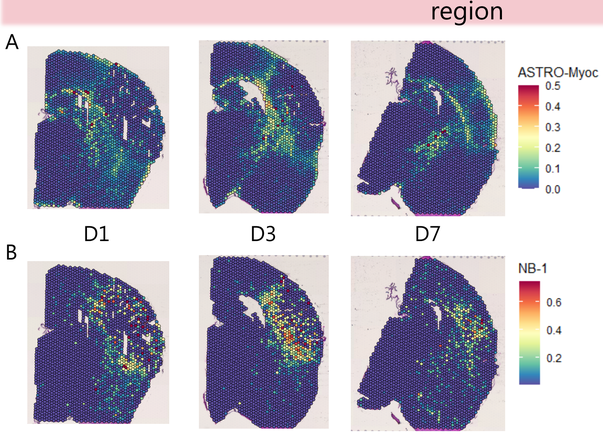

Fig. 5. Deconvolution of spots for known cell types based on public database. Spots were deconvoluted using RCTD algorithm[1] using database obtained from mousebrain.org[2]. Plots are showing cell types present in healthy mouse brain which are localized closed to the lesion. (**A**) Localization of Myoc[+]/Gfap[+] astrocytes in glial scar. (**B**) Localization of cortical neuroblastema cells around lesion. Scale bar is showing percentage of cells in spots calculated using deconvolution algorithm.

Integration of snRNA-Seq and spatial transcriptomic data

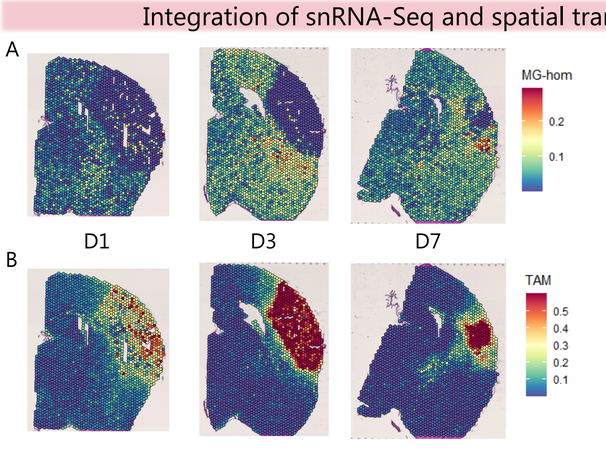

Fig. 6. Deconvolution of spots for cell subpopulations identified in this work. Spots were deconvoluted using RCTD algorithm[1] using our snRNA-Seq data as reference. (**A**) Localization of homeostatic microglia in healthy brain tissue. (**B**) Localization of trauma associated microglia in lesion and glial scar. Scale bar is showing percentage of cells in spot calculated using deconvolution algorithm.

Conclusion

We identified novel subpopulations forming during ischemic injury and described their localization and dynamics in the brain. The results are currently validated and extended by additional analysis.

Future plans

- single-cell RNA-Seq to strengthen the identification of ischemia-specific subpopulations and to improve deconvolution results
- spatial transcriptomics from control and day 7 after the injury (localized deeper inside the lesion)
- integrative analysis (cell-cell communication, bulk RNA-seq deconvolution, meta-analysis) and network analysis
- identification of targets for therapeutic intervention and their manipulation

References

1 - Cable et al., Robust decomposition of cell type mixtures in spatial transcriptomics. Nature Biotechnology, 2021.
2 - Zeisel et al., Molecular architecture of the mouse nervous system. Cell, 2018.

Funding

This study was supported by Czech Science Foundation (20-05770S) and institutional support (RVO 86652036).